JOURNAL OF AIRCRAFT
Vol. 45, No. 1, January–February 2008

Effects of Bearing Friction of a Free-to-Roll Rig on Transonic Lateral Aerodynamics

C. Edward Lan* and Silvia Bianchi†
University of Kansas, Lawrence, Kansas 66045
and
Jay M. Brandon‡
NASA Langley Research Center, Hampton, Virginia 23681

DOI: 10.2514/1.30387

Tare test data of a free-to-roll test rig with wind off are analyzed for the bearing friction by a method of differential corrections. The resulting data set is extended to transonic wind-on test conditions in oscillation frequency, amplitude, and normal force by assuming the friction coefficient to be inversely proportional to the frequency. The extended set of data is employed to establish a numerical model through a fuzzy logic algorithm. Some results showing the effects of frequency, amplitude, and normal force on the friction torque are illustrated in the paper. The predicted friction torque is then removed from the balance readings of rolling moments in the free-to-roll testing. Results of data analysis for the F-18C and F-16C models indicate that bearing-friction torques have very significant effects on the measured or experimentally determined roll damping. Without friction correction, the measured roll damping would be too small and, in some cases, even incorrect in sign. The effect of friction torque on the dihedral effect tends to be minor. Exceptions to these results appear when the configuration exhibits unstable roll damping in transonic flow.

Nomenclature

A	=	oscillation amplitude
b	=	wing span
C_l	=	rolling moment coefficient (rolling moment/$\bar{q}Sb$)
$C_{l\beta}$	=	$\partial C_l/\partial\beta$
C_{lp}	=	$\partial C_l/\partial(pb/2V)$
F	=	ratio of frequencies
I_x	=	moment of inertia about the rotation axis
k	=	spring constant in a rolling equation of motion
k_r	=	reduced frequency, $\omega b/(2V)$
M	=	Mach number
$\bar{q}$	=	dynamic pressure
R	=	multiple correlation coefficient
S	=	wing area
t	=	time
V	=	airspeed
α	=	angle of attack
β	=	sideslip angle
δ_{le}	=	leading-edge flap deflection angle
δ_{te}	=	trailing-edge flap deflection angle
δ_a	=	aileron deflection angle (symmetrically deployed)
θ	=	pitch angle
μ	=	friction coefficient
τ	=	friction torque
ϕ	=	roll angle
ψ	=	phase angle
ω	=	oscillation frequency

Presented as Paper 6490 at the AIAA Atmospheric Flight Mechanics Conference and Exhibit, Keystone, CO, 21–24 August 2006; received 11 February 2007; accepted for publication 14 September 2007.

*J. L. Constant Distinguished Professor, Department of Aerospace Engineering. Associate Fellow AIAA.
†Graduate Research Assistant, Department of Aerospace Engineering.
‡Aerospace Engineer, Flight Dynamics Branch. Associate Fellow AIAA.

I. Introduction

RECENTLY, extensive free-to-roll (FTR) testing in transonic flow conditions has been conducted to identify flight dynamic parameters that can predict various flight deficiencies [1]. However, the magnitude of bearing friction under test conditions is difficult to estimate, and so friction effects on the measured aerodynamic characteristics are usually not adequately evaluated. The importance of bearing friction in a free-to-roll test rig has been analyzed in the past. Researchers discovered from wind-tunnel test results on a delta wing model with a regular bearing at low speeds that wing rock started 7 deg lower in the angle of attack when compared with the flight data. However, when the air bearing was used, the wing rock occurred at 2 deg higher in angle of attack [2]. Although the bearing friction may not be the only factor affecting the discrepancy mentioned earlier, its impact has not been further evaluated in the previous research. During the development of the transonic free-to-roll rig for the Abrupt Wing Stall Program [3], the difficulty of determining the effect and numerical significance of the role of bearing friction emerged. Rolling friction was estimated from the FTR rig by pendulum tests with and without a model mounted on the rig. Additional values were recorded during wind-tunnel tests, with a model installed by measuring the rolling moments from an internally mounted balance and comparing with the calculated rolling moments based on the roll acceleration of the model. These estimates showed some variation of friction between runs and some differences with loads on the rig. The data across the range of conditions evaluated resulted in a range of friction factors [3]. Recently, a group of researchers from the United Kingdom, Italy, Germany, and the Netherlands also attempted to determine the magnitude of bearing friction [4]. After a considerable effort was expended, no accurate model for the friction could be obtained. The data were shown to have a strong dependence on time and temperature. Furthermore, the degree of repeatability was poor.

In this paper, estimation of the friction torque will be based on the results of wind-off pendulum test data. These data were obtained within a small range in normal forces and frequency. To extend applicability of these data to the wind-on transonic testing conditions, the data ranges in oscillation frequencies, amplitudes, and magnitude of normal forces must be largely expanded. The balance readings of the rolling moment coefficient are then corrected with the predicted friction torques, with the corrected data being

modeled through a fuzzy logic algorithm. The final numerical models for the rolling moment coefficient are then used to calculate the roll-damping derivatives and the dihedral effect.

II. Test Data

Free-to-roll tests were conducted in the NASA Langley 16-ft transonic wind tunnel using scale models. The free-to-roll (FTR) test technique consists of mounting the model and balance onto a test rig with bearings that enable it to be unconstrained in the body-axis roll degree of freedom. Figures 4 and 5 in [3] show a cross-sectional drawing of the bearings. The rig had two sets of bearings: a set of needle bearings and a set of spherical bearings to react to the loads and minimize the friction. The FTR test rig is also equipped with a brake system to allow the model to be positioned at initial nonzero roll angles and then released to study the resulting motions. The brake can also automatically stop the motions if they build up to beyond a preset maximum-allowable amplitude. During the testing, time-history recordings of the forces and moments from the internally mounted balance and the roll position of the model are recorded. Tests were conducted with several different airplane configurations; however, results of two configurations will be presented in these analyses: a 6%-scale F-18C model and a 6.67%-scale F-16C model.

Friction was determined in the tare runs with wind off by using the roll-angle time history resulting from a release of the models with counterweights from an initial angular displacement. The counterweights are used to lower the center of gravity of the assembly off the rotational axis. Most data analyzed are from the tare runs obtained from the various test models. Two runs with only the counterweights, but without any aircraft model, are also included. In all, there are 15 sets of data used.

The friction μ is assumed to depend on the frequency ω, oscillation amplitude A, and normal force (or weight in the tare runs). In the tare runs, the values of both frequency and weight are very limited, whereas in the free-to-roll testing at a transonic speed, the frequency can vary widely and the normal force can reach a few thousand pounds, both much larger than the tare values.

To avoid too much numerical extrapolation, additional data points are generated by a similarity concept. For this purpose, the equation of motion of the test rig is taken to be

$$I_x \frac{\mathrm{d}^2\phi}{\mathrm{d}t^2} + \mu \frac{\mathrm{d}\phi}{\mathrm{d}t} + k\phi = 0 \tag{1}$$

Equation (1) is nondimensionalized with

$$\bar{t} = \omega t$$

to give

$$\frac{\mathrm{d}^2\phi}{\mathrm{d}\bar{t}} + \left(\frac{\mu}{I_x\omega}\right)\frac{\mathrm{d}\phi}{\mathrm{d}\bar{t}} + \frac{k}{I_x\omega^2}\phi = 0 \tag{2}$$

By equating the similarity parameter $\mu/I_x\omega$ for two different test conditions with the same amplitude, we obtain

$$\mu_2 = \mu_1 \frac{I_{x2}}{I_{x1}}\frac{\omega_2}{\omega_1} \tag{3}$$

A reasonable assumption from [5] indicated that

$$\mu_2\omega_2 = \mu_1\omega_1 \tag{4}$$

Combining Eqs. (3) and (4), we find that

$$\frac{I_{x2}}{I_{x1}} = \frac{\omega_1^2}{\omega_2^2} \tag{5}$$

Note that Eq. (5) can also be obtained if we assume that k in Eq. (2) remains the same for the two different test conditions. If we assume that I_x is proportional to weight w, then

$$\frac{w_2}{w_1} = \frac{I_{x2}}{I_{x1}} \tag{6}$$

In summary, we have the following relations for data extrapolation, with f being the desirable frequency ratio for data extrapolation:

$$f = \frac{\omega_2}{\omega_1} \tag{7}$$

$$\mu_2 = \frac{\mu_1}{f} \tag{8}$$

$$w_2 = \frac{w_1}{f^2} \tag{9}$$

Equation (8) gives the friction torque in ft · lb per rad/s. In the present application, the friction torque in ft · lb is preferred, which is given next, noting that $\phi_1 = \phi_2$ for a constant amplitude:

$$\tau_2 = \mu_2 \mathrm{d}\phi_2/\mathrm{dt}_2 = (\mu_1/\mathrm{f})(\mathrm{d}\phi_1/\mathrm{dt}_1)\mathrm{f} = \mu_1(\mathrm{d}\phi_1/\mathrm{dt}_1) = \tau_1 \tag{10}$$

In other words, the dimensional friction torque is not changed between the two cases under consideration, based on the assumption of Eq. (4). Physically, the present friction model implies that if the frequency is increased, then the friction coefficient is decreased [Eq. (8)], but the roll rate would be higher, with the amplitude being fixed. As a result, the friction torque remains unchanged [Eq. (10)].

III. Method of Analysis for Dynamic Friction

The solution of Eq. (1) can be shown to be

$$\phi = A\exp\left(-\frac{\mu}{2I_x}t\right)\cos(\omega t + \psi) \tag{11}$$

For a given set of data in $[t, \phi]$, the unknowns in Eq. (11) to be estimated are A, $a = \mu/2I_x$, ω, and ψ. Initially, these are estimated by minimizing

$$J = \sum(\phi_i - \phi)^2 + \sum\left(\frac{\mathrm{d}\phi_i}{\mathrm{d}t} - \frac{\mathrm{d}\phi}{\mathrm{d}t}\right)^2 \tag{12}$$

where ϕ_i are data points. Once the initial estimates are obtained, the results are further refined by using the following method of differential corrections:

$$S = \sum\left(\phi_j + \frac{\partial\phi_j}{\partial a}\Delta a + \frac{\partial\phi_j}{\partial\omega}\Delta\omega + \frac{\partial\phi_j}{\partial\psi}\Delta\psi - \phi_i\right)^2 = \min \tag{13}$$

In Eq. (13), ϕ_j is the estimate and ϕ_i are the data. Equation (13) is differentiated with respect to the Δ terms, and the first derivatives are then set to zero, to result in a set of linear algebraic equations for the Δ terms. It should be noted that the amplitude A is not varied in this second step. Once these Δ terms are computed, the unknown parameters are updated as

$$a = \frac{\mu}{2I_x} = a_j + \Delta a \qquad \omega = \omega_j + \Delta\omega \qquad \psi = \psi_j + \Delta\psi$$

This process is repeated until the Δ terms are on the order of 10^{-10}.

IV. Modeling

The main challenge in modeling the friction torque in the free-to-roll testing is that the available test data are confined within the narrow ranges of frequencies (3–4.4 rad/s) and weights or normal forces (55–560 lb). However, in the transonic tests, the frequency could exceed 10 rad/s, and the normal force could exceed more than several thousand pounds. Therefore, a robust extrapolation scheme is necessary. In the present application, the fuzzy logic scheme developed for aerodynamic modeling will be used [6]. The fuzzy logic modeling technique is a nonlinear multivariable approximation scheme reliable for interpolation. Although the present fuzzy logic

modeling technique can extrapolate the test data to outside, but close to, the experimental range reasonably well, the results would not be reliable without additional *anchoring* points that are far away from the experimental range. These additional data points are estimated with the concept indicated in Eq. (4). Furthermore, when the frequency is zero, the dynamic friction torque is also assumed to be zero (taken to be 0.01 for a better numerical convergence). In the numerical model, the influencing parameters on the friction torque are taken to have ranges of frequency of 0 to 35.0 rad/s, amplitude of 0 to 150.0 deg, and normal force of 0 to 4500.0 lb

The numerical values represent the desired ranges in the numerical model. There are only 15 points in the available data set (see [7] for details). The extended data points are set up by applying Eqs. (7–9) to the available data set and choosing points over desired ranges in frequency, amplitude, and weights. It is not necessary to have equal spacing in these variables among these extra points. After each modeling run, the predicted results over the desired ranges in frequency, amplitude, and weights are examined to determine if additional data points are needed. The criteria for adding data points are 1) at the lower ends of variable values, the predicted friction torques should not be negative and 2) at the high ends of variable values, the predicted results should be minimized, whereas the squared correlation coefficient R^2 is maximized. The final R^2 value in the friction model is 0.9807. At the same time, the predicted value of torque at a frequency of 10.5 rad/s and weight of 1000 lb (serving as the control condition) will not decrease further. In the final results reported here, this control condition varies by less than 0.05% over 200,000 iterations in modeling. It should be noted that friction torque theoretically should be dependent on temperature, because the bearing may expand or contract if the temperature increases or decreases. However, because of a lack of data, temperature is not used as an influencing variable in the present study.

By using the measured roll-angle time history ϕ(t) and fitting each segment of 20 points (equivalent to 0.2 s) with a harmonic variation, the local oscillation frequency can be estimated [8]. The window size of 20 points is chosen in [8] to be the best. If it is less than 20 points, the numerical convergence in determining the frequency by a least-squares method gets worse. But if it is larger than 20 points, then the computing time would be increased. The needed $\mathrm{d}\phi/\mathrm{dt}$ is estimated with a monotone cubic spline [9]. The vector sum of the measured normal load and the model weight plus counterweight provides the total normal force (to be simply called the normal force) acting on the bearing. Based on the estimated amplitude of the equivalent harmonic oscillation, frequency, and the normal force, the friction torque can be estimated. The equation of motion with the wind on is assumed to be of the form

$$I_x \frac{\mathrm{d}^2\phi}{\mathrm{d}t^2} + \mu \frac{\mathrm{d}\phi}{\mathrm{d}t} = C_l \bar{q} S b \tag{14}$$

where the right-hand side is measured by the balance. Therefore, the balance measurement must be subtracted by $\mu\,\mathrm{d}\phi/\mathrm{dt}$. In addition, the modeled friction torque is always positive. In application, it should have the same sign as $\mathrm{d}\phi/\mathrm{dt}$.

During roll oscillations, α and β will vary in accordance with the following kinematic relations:

$$\tan\alpha = \cos\phi \tan\theta \tag{15}$$

$$\sin\beta = \sin\phi \sin\theta \tag{16}$$

In the present investigation, the rolling moment coefficient C_l is considered to be dependent on the following motion variables: angle of attack α, angle of sideslip β, roll angle ϕ, roll rate p, reduced frequency k_r [$\omega b/(2V)$], Mach number M, time rate of the angle of attack $\dot{\alpha}$, and time rate of the sideslip angle $\dot{\beta}$. The fuzzy logic algorithm uses both the least-squares errors and the multiple correlation coefficients to determine the most suitable model [6]. After a numerical model of the rolling moment coefficient (i.e., the fuzzy logic model) is obtained, all derivatives are calculated by using the numerical model through a central-difference scheme. For example, C_{lp} is evaluated as $\Delta C_l/\Delta(pb/2V)$, with all other variables remaining unchanged from their instant values.

V. Results and Discussion

A. Friction Models

The available data model was based on 15 data points. On the other hand, the final model is based on the available data points plus additional extended data. The trend of variation in three cases (variation in frequency, weight, and oscillation amplitude) will be presented. The effect of frequency is illustrated in Fig. 1. It shows that the higher the frequency, the larger the friction torque when the amplitude is greater than 10 deg. The torque is also increased with weights and amplitudes. Using only the available 15 data points (in symbols) is shown to be inadequate in producing the correct trend. Note that all continuous curves are based on the numerical model (i.e., the fuzzy logic model).

The effect of weights at constant frequency and amplitude is illustrated in Fig. 2. The reason for a dip between $w = 900$–1500 lb is not known.

Finally, the effect of oscillation amplitude is illustrated in Fig. 3. As the amplitude of oscillation increases, the friction torque mostly tends to increase as well.

B. Lateral Aerodynamics

Two configurations are investigated in this paper: the F-18C and the F-16C. In addition, only those cases that exhibited generally damped behaviors in the transonic free-to-roll tests will be examined. More than 400 test runs for each model were conducted in a transonic tunnel. However, only some cases representing various test conditions [such as the initial angle of attack, Mach number, and the settings of leading edge, trailing edge, and aileron deflections

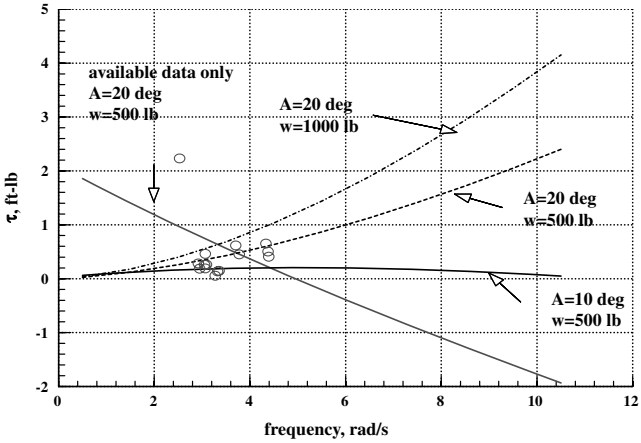

Fig. 1 Effect of frequency on the friction torque; *A* is the amplitude in degrees.

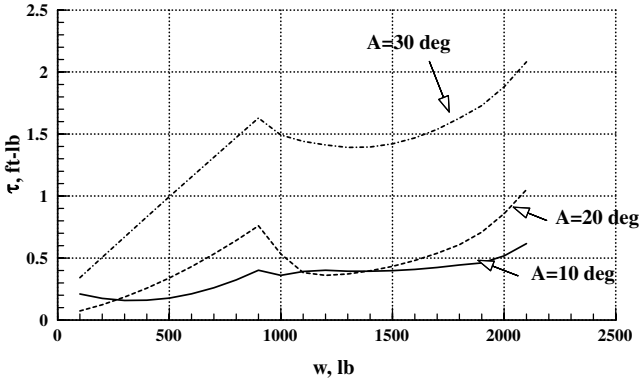

Fig. 2 Effect of weights on friction torque at a frequency of 3 rad/s.

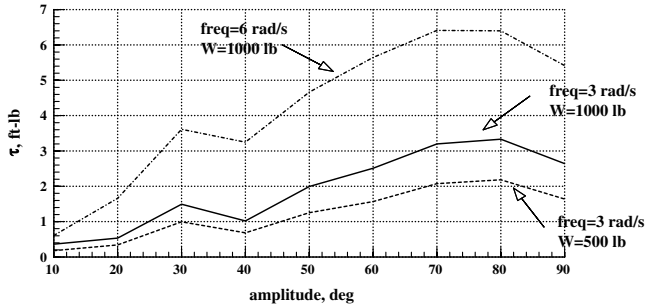

Fig. 3 Effect of oscillation amplitude on friction torque.

(deployed symmetrically)] will be reported here. The main purpose is to obtain the quantitative magnitude of the friction effects on the roll damping and dihedral effect in transonic free-to-roll tests. All roll-damping and dihedral-effect derivatives are calculated as averages over the last portion of the time history with the motion sufficiently damped, except as noted. In addition, they are always calculated as the derivatives at the local, or instantaneous, conditions (i.e., nonzero values of roll angle and roll rate), not about the trim conditions (i.e., zero values of roll angle and roll rate), as done conventionally.

1. F-18C Model

All test runs of this model under analysis are characterized by the fact that an initial angle of attack or pitch angle θ is set, the model is rolled to an initial roll angle, and the brake on the FTR rig is then engaged. At the beginning of the data run, the brake is released and data are obtained while the ensuing roll motions are damped out. This mode of operation of the FTR rig is called the "ϕ-release technique." Nine runs corresponding to various flow conditions are analyzed, but only four sets of figures showing different motion characteristics will be presented here. Results of each run will be presented separately and a final summary will be available at the end.

It should be noted that the time histories for both cases with and without friction corrections are similar, as can be seen from the following figures, except that one may be shifted with respect to the other. However, right after release, the initial transient response can be quite different.

a. Model F-18C, Run 450. In this run, the test conditions are $M = 0.85$, the pitch angle was 13.69 deg, and the settings of leading edge, trailing edge, and aileron extension were given by $\delta_{\text{le}}/\delta_{\text{te}}/\delta_a = 10/12/0$ deg. In this run, the variation of derivatives is not completely stabilized (see Fig. 4; in particular, the roll damping). The latter is evaluated as the average of values over $t \geq 20$ s.

Note that in the initial part of the time history with no noticeable motion, the measured rolling moment represents the static lateral aerodynamics induced by the asymmetrical effects of shock and leading-edge-extension (LEX) vortices in sideslip. Static friction may contribute a small amount. Because all derivatives are calculated at the local, or instantaneous, conditions, the calculated C_{lp} represents the roll damping at $\phi \approx 60$ deg, evaluated based on the general trend in the established roll aerodynamic model. The roll rates assumed in the central-difference calculation are $\Delta p = \pm 1$ deg/s. After the rolling motion begins ($t > 1.5$ s in Fig. 4c), C_{lp} and $C_{l\beta}$ are evaluated at varying α and β because of changing roll angle and are not constant. The average lateral derivatives for run 450 of the F-18C model are 0.005551 for $C_{l\beta}$ and -0.20698 for C_{lp} with friction correction and -0.03739 for $C_{l\beta}$ and 0.349347 for C_{lp} without friction correction.

The nonconstant values of these derivatives may also indicate nonlinear behavior of the aerodynamics, such as the effect of β on roll damping in wing rock. If these derivatives in large-amplitude motions are to be estimated, values at approximately the same roll angle in the initial free part of the run can be averaged to provide the values of these derivatives at the corresponding α and β.

b. Model F-18C, Run 254. The value of Mach number in this case was $M = 0.8$, the pitch angle was 8.7 deg, and the settings of

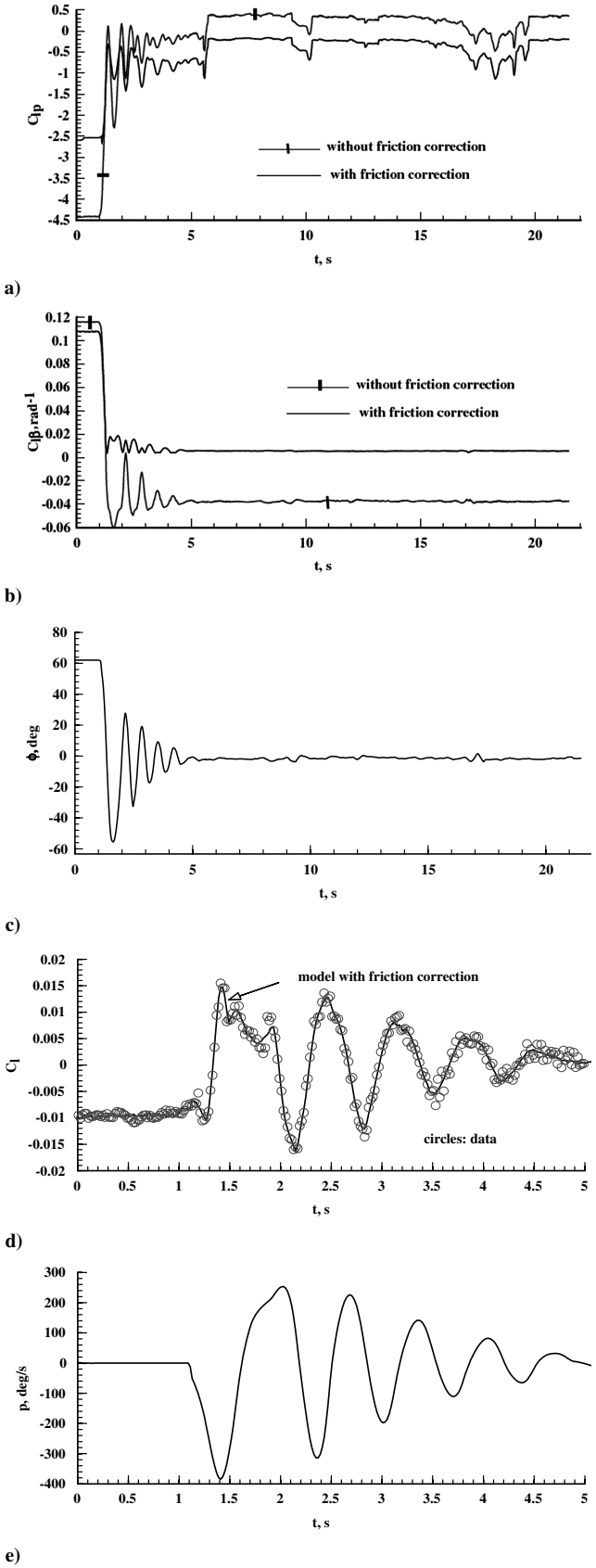

Fig. 4 Variation of aerodynamic derivatives for model F-18C, run 450; $M = 0.85$, $\theta = 13.69$ deg, $\delta_{\text{le}}/\delta_{\text{te}}/\delta_a = 10/12/0$ deg.

leading edge, trailing edge, and aileron deflection angles were given by $\delta_{\text{le}}/\delta_{\text{te}}/\delta_a = 6/8/0$ deg. The detailed results are presented in Fig. 5. The average lateral derivatives for run 254 of the F-18C model are -0.07852 for $C_{l\beta}$ and -0.52294 for C_{lp} with friction correction

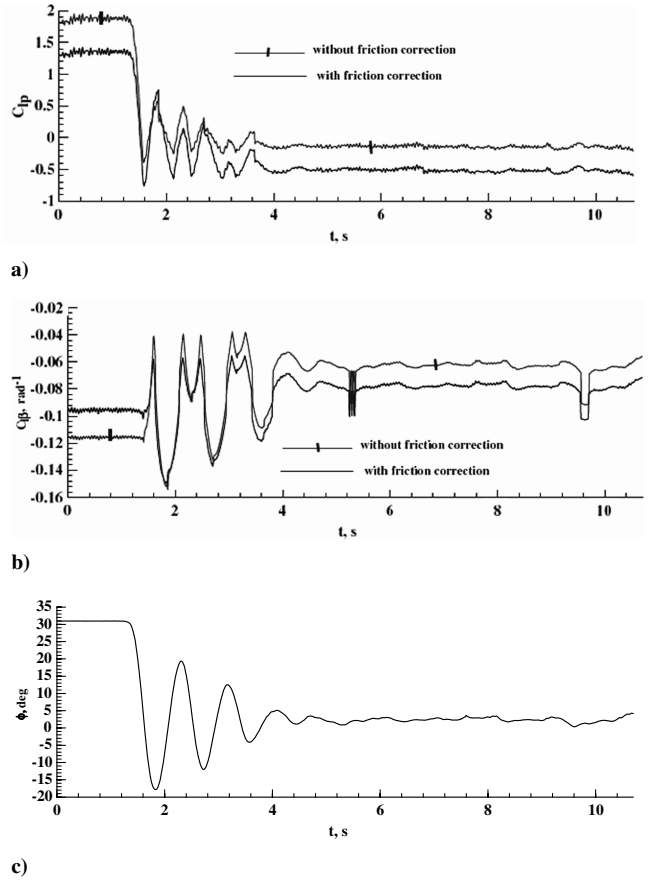

Fig. 5 Variation of aerodynamic derivatives for model F-18C, run 254; $M = 0.8$, $\theta = 8.7$ deg, and $\delta_{le}/\delta_{te}/\delta_a = 6/8/0$ deg.

and -0.06333 for $C_{l\beta}$ and -0.14628 for C_{lp} without friction correction.

It is seen that without the friction correction, the magnitude of stable roll damping is reduced. At the same time, the stable dihedral effect is also slightly reduced. Because the stable dihedral effect serves as the system stiffness in a linear theory, its magnitude is naturally affected by damping, just like the system frequency being affected by damping to result in a damped frequency. Of course, we have to bear in mind that the transonic aerodynamics is nonlinear in general. The derivatives are calculated as the average over $t \geq 6$ s.

c. Model F-18C, Run 291. In this run, the test conditions are $M = 0.85$, the pitch angle was 9.9 deg, and the settings of leading edge, trailing edge, and aileron deflection angles were given by $\delta_{le}/\delta_{te}/\delta_a = 6/8/0$ deg. The detailed results are presented in Fig. 6 and the average is taken over $t \geq 6$ s. The average lateral derivatives for run 291 of the F-18C model based on averaged values are -1.2699 for $C_{l\beta}$ and 0.276643 for C_{lp} with friction correction and -0.06865 for $C_{l\beta}$ and 0.00995 for C_{lp} without friction correction. The lateral derivatives for run 291 of the F-18C model at the end of the run are -1.3069 for $C_{l\beta}$ and -0.0396 for C_{lp} with friction correction and -0.0507 for $C_{l\beta}$ and -0.1328 for C_{lp} without friction correction.

From the time history of the derivatives, we notice that no clear stabilized state is reached. The lateral motion is dominated by the dihedral effect, and the roll damping is relatively small, even though it is unstable. In fact, if we compare the last values, instead of taking the average, then we would have what was presented in the preceding paragraph.

d. Model F-18C, Run 483. In this run, the test conditions are $M = 0.9$, the pitch angle was 10.06 deg, and the settings of leading edge, trailing edge, and aileron extension were given by $\delta_{le}/\delta_{te}/\delta_a = 10/12/0$ deg. The detailed results are presented in Fig. 7. The average lateral derivatives for run 483 of the F-18C model are 0.140884 for $C_{l\beta}$ and 0.924069 for C_{lp} with friction correction and 0.266378 for $C_{l\beta}$ and 1.2194 for C_{lp} without friction correction.

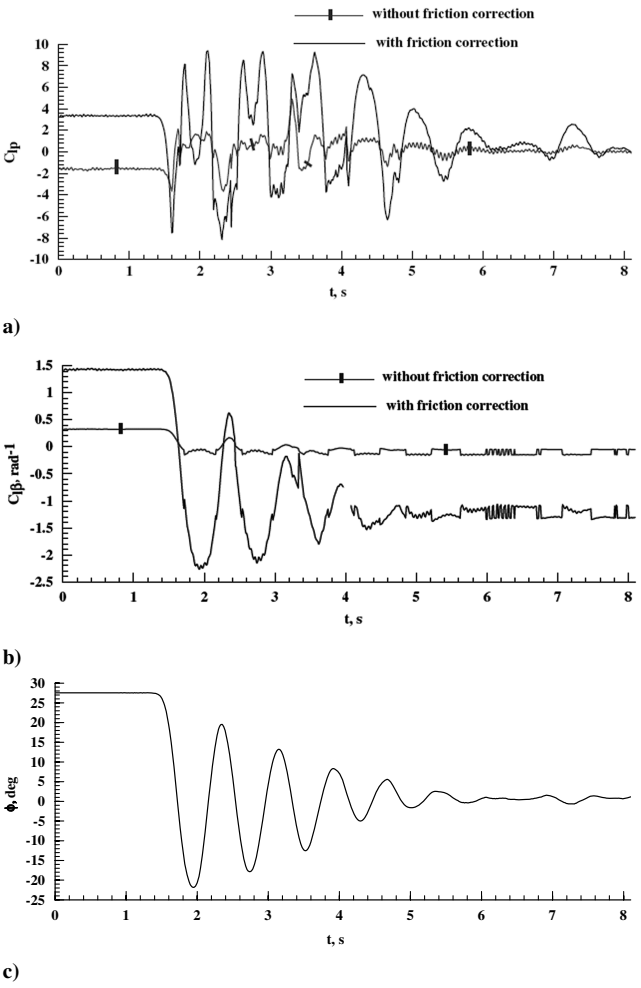

Fig. 6 Variation of aerodynamic derivatives for model F-18C, run 291; $M = 0.85$, $\theta = 9.9$ deg, and $\delta_{le}/\delta_{te}/\delta_a = 6/8/0$ deg.

As shown in Fig. 7a, right after release, the roll damping is large and stable, and so the rolling motion should be highly damped. However, the converged roll angle is not zero. In appearance, Fig. 7c indicates convergence in the rolling motion. However, the calculated roll damping is unstable. The inconsistency is explained in Fig. 8, in which it shows that the motion is not completely converged and continues to oscillate around a nonzero roll angle. Again, the behavior of predicted derivatives in the first 1.5 s is caused by static lateral aerodynamics in sideslip.

e. Summary of F-18C Test Results. A summary of all test runs analyzed for F-18C, test 564, is given in Table 1. As expected, the damping coefficient C_{lp} is more sensitive to friction than the dihedral effect $C_{l\beta}$. When the predicted derivatives are unstable (i.e., positive), yet very little rolling motion remains, the situation can be explained by the existence of static friction. The effect of leading-edge flap deflection tends to reduce the dihedral effect (i.e., more positive), but not the roll damping, as can be seen from runs 449 and 561 and runs 381 and 556. The trend of lateral derivatives can be summarized as follows:

For $C_{l\beta}$, the values obtained without friction correction are always slightly more positive than those with friction correction, except for the case of run 450. In this latter case, the motion has not completely converged and is dominated by roll damping.

For C_{lp}, the values obtained from the model without friction correction are always higher (i.e., more positive) than those with friction correction, except run 291. In the latter case, the motion has again not completely converged and is dominated by dihedral effect.

2. *Model F-16C*

For this model, all the test runs selected are again characterized by having different pitch angles. There are only settings of leading-edge

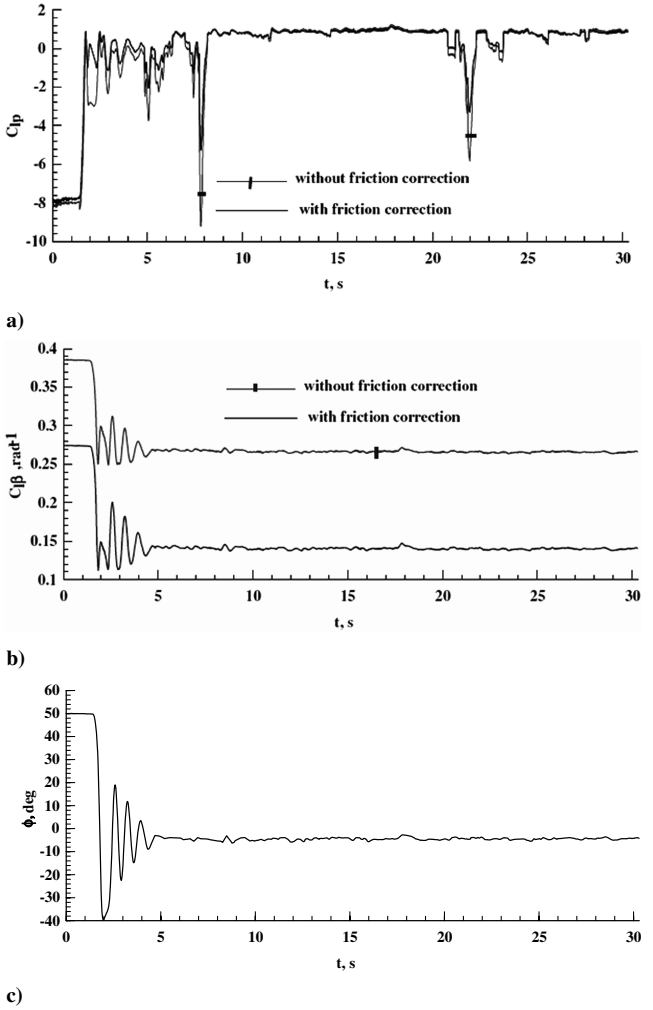

Fig. 7 Variation of aerodynamic derivatives for model F-18C, run 483; $M = 0.9$, $\theta = 10.06$ deg, and $\delta_{le}/\delta_{te}/\delta_a = 10/12/0$ deg.

and trailing-edge flap angles. The aileron is not deflected. Six sets of test data are analyzed. However, only three of them will be presented in detail here. Again, all final magnitudes of derivatives are calculated as the average over a time period within which the variation is regarded as small.

a. Model F-16C, Run 84. The test conditions for this case are $M = 0.8$, $\theta = 10.08$ deg, and $\delta_{le}/\delta_{te} = 0/0$ deg. The detailed results of the lateral derivatives for run 84 of the F-16C model are presented in Fig. 9 and the average values are -0.18629 for $C_{l\beta}$ and -1.36141 for C_{lp} with friction correction and are presented in Fig. 9, and the average values are -0.17726 for $C_{l\beta}$ and 0.075815 for C_{lp} without friction correction. In this case, the motion is relatively well damped to result in expected values for the roll damping and dihedral effect. That is, without friction correction, the estimated result for damping would not be correct.

b. Model F-16C, Run 198. The test conditions for this run are $M = 0.8$, $\theta = 10.06$ deg, and $\delta_{le}/\delta_{te} = 5/0$ deg. The average results for the lateral derivatives for run 198 of the F-16C model are -0.05368 for $C_{l\beta}$ and -0.33258 for C_{lp} with friction correction and are presented in detail in Fig. 10, and the average values are -0.03828 for $C_{l\beta}$ and -1.27426 for C_{lp} without friction correction.

The only difference in run 198 compared with the previous one (run 84) is the leading-edge flap angle. With $\delta_{le} = 5$ deg, the span loading is decreased so that both the dihedral effect and roll damping are reduced.

c. Model F-16C, Run 312. This case is characterized by the following test conditions: $M = 0.9$, $\theta = 4.1$ deg, and $\delta_{le}/\delta_{te} = 10/0$ deg. The average results for the lateral derivatives for run 312 of

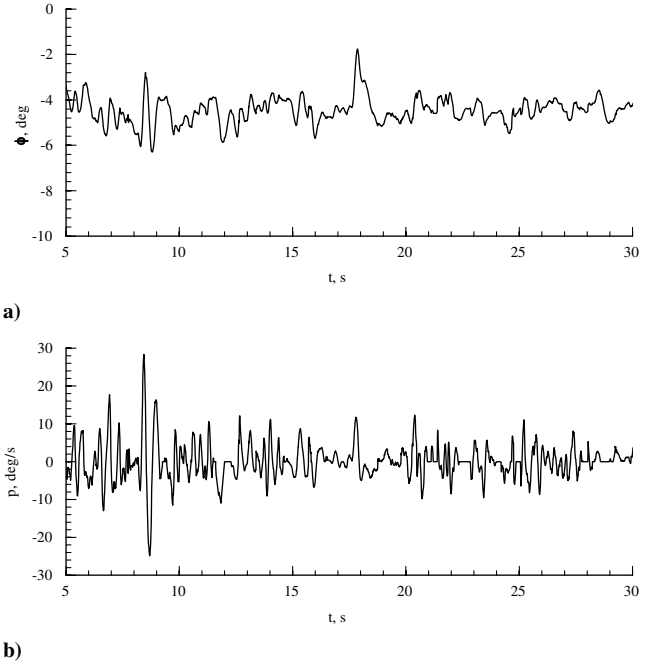

Fig. 8 Enlarged plot of motion for model F-18C, run 483 with friction corrections; $M = 0.9$, $\theta = 10.06$ deg, and $\delta_{le}/\delta_{te}/\delta_a = 10/12/0$ deg.

the F-16C model are -0.17322 for $C_{l\beta}$ and -0.24201 for C_{lp} with friction correction and are presented in detail in Fig. 11, and the average values are -0.21322 for $C_{l\beta}$ and 0.088931 for C_{lp} without friction correction.

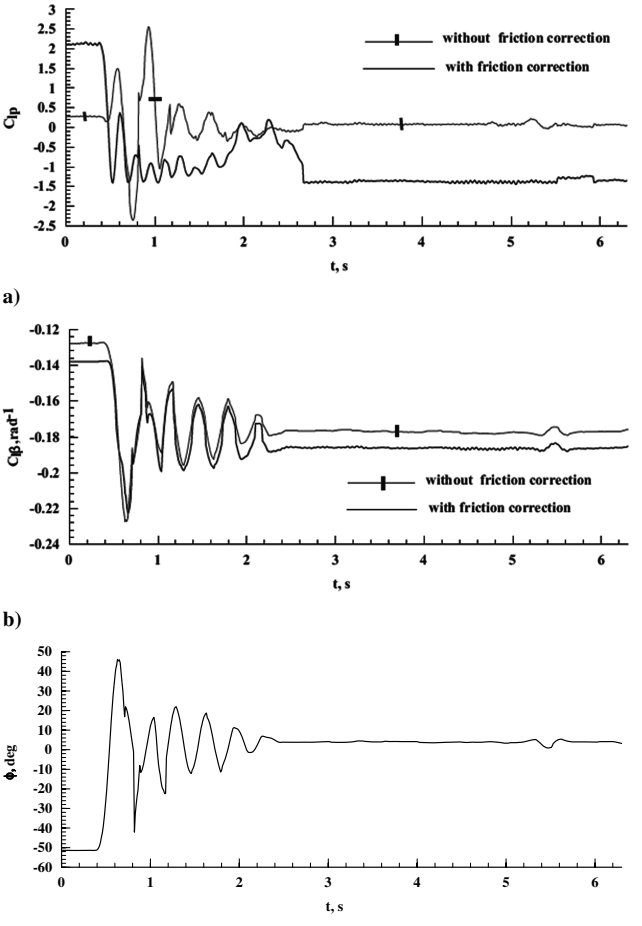

Fig. 9 Variation of aerodynamics derivatives for model F-16C, run 84; $M = 0.8$, $\theta = 10.08$ deg, and $\delta_{le}/\delta_{te} = 0/0$ deg.

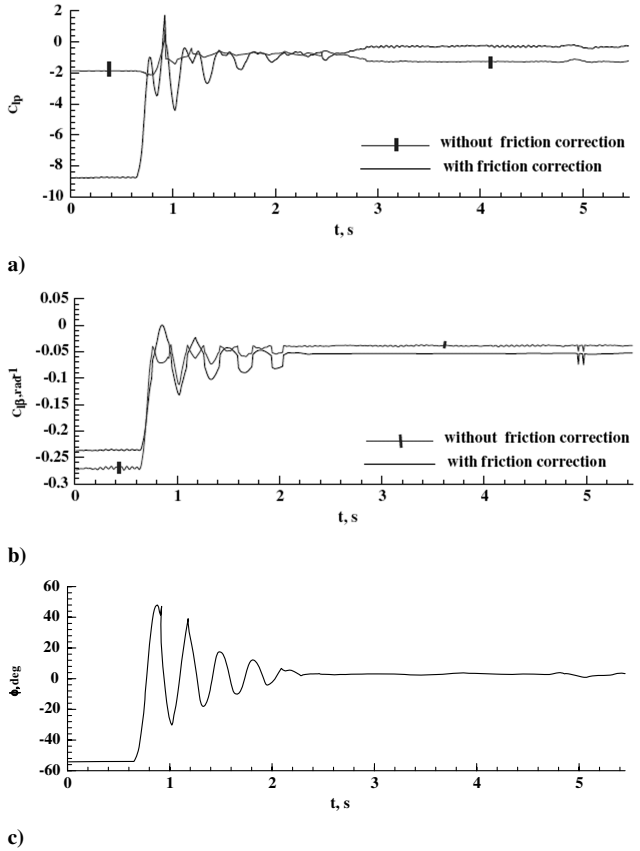

Fig. 10 Variation of aerodynamics derivatives for model F-16C, run 198; $M = 0.8$, $\alpha_i = 10.06$ deg, and $\delta_{le}/\delta_{te} = 5/0$ deg.

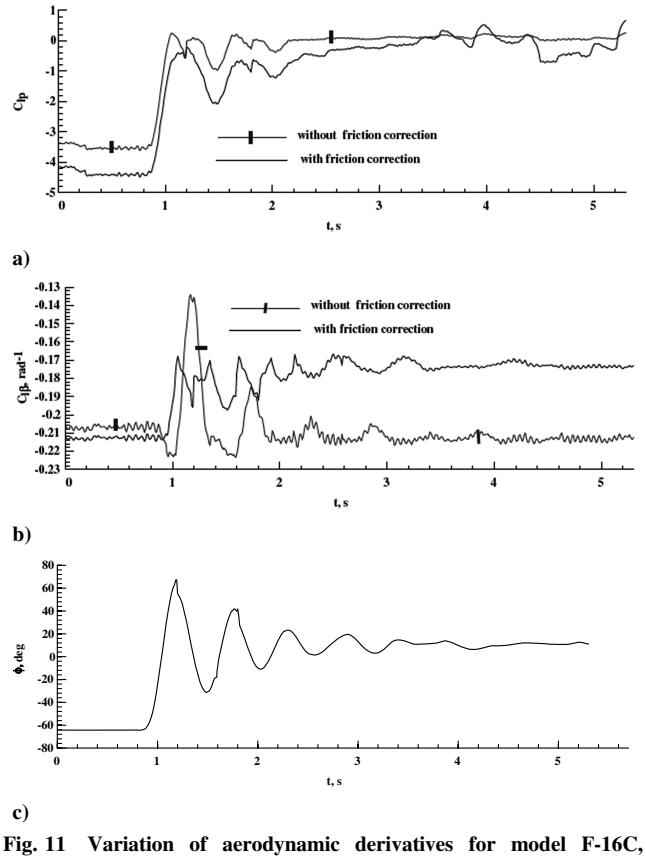

Fig. 11 Variation of aerodynamic derivatives for model F-16C, run 312; $M = 0.9$, $\theta = 4.1$ deg, and $\delta_{le}/\delta_{te} = 10/0$ deg.

In run 312, again, the variation of the derivatives is not completely stabilized. With $\delta_{le} = 10$ deg, the magnitude of both the dihedral effect and roll damping would be reduced when compared with the clean configuration, but both derivatives remain stable.

d. Summary of F-16C Test Results. A summary of the test runs analyzed for F-16C, test 567, is given in Table 2. For the model of F-16C, the effect of friction is similar to that for the model of F-18C. In particular, for C_{lp}, the values obtained from the model without friction correction are always higher (i.e., more positive) than those with friction correction, except run 198.

For $C_{l\beta}$, the trend is not as clear-cut, depending on the magnitude of damping. In most cases, the values for the model without friction correction are higher (i.e., more positive) than those with the friction correction, except at a Mach number of 0.9, when the opposite trend is true.

Table 1 Summary of lateral derivatives for the F-18C model

Run	Parameters	Mach	Pitch angle	With friction correction		Without friction correction	
				$C_{l\beta}$	C_{lp}	$C_{l\beta}$	C_{lp}
254	$\delta_{le}/\delta_{te}/\delta_a = 6/8/0$ deg	0.8	8.7	−0.07852	−0.52294	−0.06333	−0.14628
291	$\delta_{le}/\delta_{te}/\delta_a = 6/8/0$ deg	0.85	9.9	−1.2699	0.276643	−0.06865	0.00995
331	$\delta_{le}/\delta_{te}/\delta_a = 6/8/0$ deg	0.9	10.48	0.065688	−0.7239	0.073679	−0.2881
381	$\delta_{le}/\delta_{te}/\delta_a = 10/12/0$ deg	0.8	8.89	−0.10178	−0.2964	−0.07789	0.103896
449	$\delta_{le}/\delta_{te}/\delta_a = 10/12/0$ deg	0.85	12.5	−0.01215	−0.72397	−0.00408	0.215064
450	$\delta_{le}/\delta_{te}/\delta_a = 10/12/0$ deg	0.85	13.62	0.005551	−0.20698	−0.03739	0.349347
483	$\delta_{le}/\delta_{te}/\delta_a = 10/12/0$ deg	0.9	10.06	0.140884	0.924069	0.266378	1.2194
556	$\delta_{le}/\delta_{te}/\delta_a = 15/12/0$ deg	0.8	9.18	0.206294	−0.61154	0.203366	−0.36796
561	$\delta_{le}/\delta_{te}/\delta_a = 15/12/0$ deg	0.85	12.5	0.0537	−1.3348	0.089778	−0.68093

Table 2 Summary of lateral derivatives for the F-16C model

Run	Parameters	Mach	Pitch angle	With friction correction		Without friction correction	
				$C_{l\beta}$	C_{lp}	$C_{l\beta}$	C_{lp}
84	$\delta_{le}/\delta_{te} = 0/0$ deg	0.8	10.08	−0.18629	−1.36141	−0.17726	.075815
100	$\delta_{le}/\delta_{te} = 0/0$ deg	0.9	7.13	−0.20096	−0.77162	−0.2823	0.028718
198	$\delta_{le}/\delta_{te} = 5/0$ deg	0.8	10.05	−0.05368	−0.33258	−0.03828	−1.27426
217	$\delta_{le}/\delta_{te} = 5/0$ deg	0.9	7.64	−0.16107	−0.49597	−0.19207	0.121306
295	$\delta_{le}/\delta_{te} = 10/0$ deg	0.8	4.07	−0.00446	−0.76767	−0.00376	−0.44367
312	$\delta_{le}/\delta_{te} = 10/0$ deg	0.9	4.1	−0.17322	−0.24201	−0.21322	0.088931

In all cases, the leading-edge flap always reduces the magnitude of both the dihedral effect and roll damping. Without the friction correction, the measured roll damping may even have incorrect sign.

VI. Conclusions

Based on an established numerical model, it was shown that the bearing friction in a free-to-roll test rig depended nonlinearly on the oscillation frequency, oscillation amplitude, and the normal force acting on the bearing. Without the friction correction, the estimated roll damping would not be correct, not only in magnitude, but sometimes even in sign. In general, without friction correction, the predicted roll damping would be less negative (i.e., more unstable), with some exceptions. These exceptional cases were configuration-dependent: for the F-18C model, it occurred at a Mach number of 0.85, a pitch angle of 9.9 deg, and a leading-edge flap angle of 6 deg. For the F-16C model, it occurred at a Mach number of 0.8, a pitch angle of 10.05 deg, and a leading-edge flap angle of 5 deg. At a higher leading-edge flap angle but lower pitch angle, these exceptional cases did not occur. For the predicted dihedral effect, the effect of bearing friction was much smaller. In general, the values obtained without friction correction are always slightly more positive than those with friction correction, again with some exceptions. For the F-18C model, one exceptional case occurred at a Mach number equal to 0.85, a pitch angle of 13.62 deg, and leading-edge flap angle of 10 deg. For the F-16C model, the exceptional cases occurred only at a Mach number equal to 0.9.

In future research, it is recommended to acquire more data points covering a wider range of parameters for the same bearing. These additional data points can be added to the presently available database and the fuzzy logic friction model can then be retrained to improve the accuracy and reliability. The effect of bearing temperature should also be evaluated. The free-to-roll technique to acquire the lateral derivatives should also be compared with the forced oscillation technique.

Acknowledgments

This research was supported by grant NNL04AA23G from NASA Langley Research Center for the first two authors. The computing time was provided by the Center for Advanced Scientific Computing at the University of Kansas.

References

[1] Owens, D. B., Capone, F. J., Hall, R. M., Brandon, J. M., and Chambers J. R., "Free-to-Roll Analysis of Abrupt Wing Stall on Military Aircraft," *Journal of Aircraft*, Vol. 41, No. 3, 2004, pp. 474–484.

[2] Quast, T., Nelson, R. C., and Ficher, D. F., "A Study of High Alpha Dynamics and Flow Visualization for a 2.5% Model of the F-18 HARV Undergoing Wing Rock," AIAA Paper 91-3267, Sept. 1991.

[3] Capone, F. J., Owens, D. B., and Hall, R. M., "Development of a Free-to-Roll Transonic Test Capability," *Journal of Aircraft*, Vol. 41, No. 3, 2004, pp. 456–463.

[4] Arthur, M. T., Allan, M., Ceresola, K. J., Fritz, W., Boelens, O. J., and Prananta, B. B., "Exploration of the Free Rolling Motion of a Delta Wing Configuration in Vortical Flow," *Flow-Induced Unsteady Loads and the Impact on Military Applications* [CD-ROM], RTO-MP-AVT-123, NATO Research and Technology Organization, Neuilly sur-Seine Cedex, France, 25–28 Apr. 2005, Paper 14.

[5] Smith, T. L., "Dynamic Stability Measurements," Ballistic Research Labs., Rept. 1352, Aberdeen Proving Ground, MD, June 1961.

[6] Wang, Z., Lan, C. E., and Brandon, J. M., "Fuzzy-Logic Modeling of Nonlinear Unsteady Aerodynamics," AIAA Paper 98-4351, Aug. 1998.

[7] Bianchi, S., "Estimation of Nonlinear Aerodynamic Roll Model for the Identification of Uncommanded Rolling Motions," M.S. Thesis, Univ. of Kansas, Lawrence, KS, 2005; also *Masters Abstracts International*, Vol. 44-02, p. 0952, 2005.

[8] Wang, Z., Lan, C. E., and Brandon, J. M., "Unsteady Aerodynamic Effects on the Flight Characteristics of an F-16XL Configuration," AIAA Paper 2000-3910, Aug. 2000.

[9] Huynh, H. T., "Accurate Monotone Cubic Interpolation," *SIAM Journal on Numerical Analysis*, Vol. 30, No. 1, Feb. 1993, pp. 57–100. doi:10.1137/0730004